Impact of cloud radiative heating on East Asian summer monsoon circulation

2015 Environ. Res. Lett. 10 074014

(http://iopscience.iop.org/1748-9326/10/7/074014)

Environmental Research Letters

LETTER

Impact of cloud radiative heating on East Asian summer monsoon circulation

CrossMark

OPEN ACCESS

RECEIVED
25 October 2014

REVISED
25 March 2015

ACCEPTED FOR PUBLICATION
9 May 2015

PUBLISHED
17 July 2015

Zhun Guo[1,2,3], **Tianjun Zhou**[1,2], **Minghuai Wang**[3,4,5] **and Yun Qian**[5]

[1] LASG, Institute of Atmospheric Physics, Chinese Academy of Sciences, Beijing, People's Republic of China
[2] Climate Change Research Center, Chinese Academy of Sciences, Beijing, People's Republic of China
[3] Institute for Climate and Global Change Research & School of Atmospheric Sciences, Nanjing University, Nanjing, 210093, People's Republic of China
[4] Collaborative Innovation Center of Climate Change, Jiangsu Province, People's Republic of China
[5] Pacific Northwest National Laboratory, Richland, WA, USA

E-mail: zhoutj@lasg.iap.ac.cn

Keywords: East Asian summer monsoon, cloud radiative heating, numerical experiments

Abstract

The impacts of cloud radiative heating on the East Asian Summer Monsoon (EASM) over southeastern China (105°–125°E, 20°–35°N) are addressed by using the Community Atmosphere Model version 5 (CAM5). Sensitivity experiments demonstrate that the radiative heating of clouds leads to a positive effect on the local EASM circulation over southeastern China. Without the radiative heating of clouds, the EASM circulation and precipitation would be much weaker than that in normal conditions. The longwave heating of clouds dominates the changes of EASM circulation. The positive effect of clouds on EASM circulation is explained by the thermodynamic energy equation, i.e. the different heating rate between cloud base and cloud top enhances the convective instability over southeastern China, which consequently enhances updraft. The strong updraft would further result in a southward meridional wind above the center of the updraft through Sverdrup vorticity balance.

1. Introduction

East Asian Summer monsoon (EASM) has prominent impacts on the local climate of East Asia (Wang and Li 2004). In each boreal summer, the southwesterly wind along the southern flank of the western Pacific subtropical high carries moist warm air from the Pacific and meets the cold continental air mass over Southeastern China. The East Asian subtropical front is thus established, which weakens the baroclinicity significantly and increases the frequency of deep convections (Ding and Chan 2005, Wang *et al* 2008). Along the frontal zone, a significant portion of the convective precipitation extends from the Yangtze River valley eastward to Japan, due to the high occurrence frequency of deep convections (Ding and Chan 2005). Correspondingly, prevailing low clouds in winter are replaced by high clouds in summer over southeastern China, including deep cumulus and cirrus (e.g., Yu *et al* 2001, Luo *et al* 2009).

The cloud is traditionally regarded as a result of atmospheric circulation changes associated with the EASM system. It is well recognized that the latent heats released by lifting condensations lead to positive effects in the development of EASM. However, the radiative effects of clouds are somewhat overlooked. Clouds are generally thought to warm the underlying atmosphere by their greenhouse effects, and cool the atmosphere underneath the cloud and heat the cloud aloft through their reflection and absorption of shortwave radiation. Such a vertical difference in heating rates between the cloud base and cloud top is strong enough to cause convective instability in anvils (Ackerman *et al* 1988, Mather *et al* 2007). We thus hypothesize that clouds can feedback on the EASM circulation through its different radiative heating effects between the underlying air and cloud top. This hypothesis is examined by performing numerical experiments with the Community Atmosphere Model version 5 (CAM5). We show evidence that, without accounting for the cloud radiative heating, EASM circulation and monsoon precipitation would (significantly) become weaker.

Table 1. Details of senstivty experments.

Experiment	Description	Method
CNTL	Control run of CAM5	6 year run forced by climatology SST, last 5 years are used
NL	No longwave cloud radiative effect over southeastern China (105°–125°E, 20°–35°N)	Set all longwave all-sky radiative fluxes equal to their clear-sky counter parts over (105°–125°E, 20°–35°N)
NS	No shortwave cloud radiative effect over southeastern China	Same method as NL run, but for the shortwaves
NR	No net cloud radiative effect over southeastern China	Same method as NL run, but for both shortwaves and longwaves

2. Data, model and methods

The datasets used in this study consist of the following seasonally mean fields:

(1) The National Center for Environmental Prediction Department of Energy Atmospheric Model Intercomparison Project reanalysis II (NCEP2) (Kanamitsu *et al* 2002) from 1979 to 2011 is used to describe the climatological atmospheric general circulation.

(2) The CPC Merged Analysis of Precipitation (CMAP) data from 1979 to 2011 is used to describe the climatological monsoon rain band (Xie and Arkin, 1996).

(3) CloudSat and CALIPSO (Cloud-Aerosol Lidar and Infrared Pathfinder Satellite Observations) data from 2006 to 2011 are used to depict the vertical structure of cloud (Stephens *et al* 2002[6]). CloudSat, which carries the Cloud Profiling Radar with its estimated minimum detectable signal of −30 dBZ, provides reflectivity (from Level 2 CloudSat Geometrical Profiling Product) and heating rates (from Level 2 CloudSat Fluxes and Heating Rates Product) that are used in this study.

Numerical experiments are performed by using CAM5 (Neale *et al* 2011). Stratiform clouds and cumulus in CAM5 are treated by separate cloud parameterizations. The shallow cumulus scheme is described by Park and Bretherton (2009) and deep cumulus is treated by the Zhang and McFarlane scheme (Zhang and McFarlane 1995, Neale *et al* 2008). Stratiform cloud macrophysics is described by Park *et al* (2014) and Gettelman *et al* (2010). The model applies the Rapid Radiative Transfer Model for general circulation models (RRTMG) to treat the radiative transfer (Mlawer *et al* 1997, Iacono *et al* 2000).

In order to examine how the cloud radiative heating affects EASM over southeastern China, we perform three sensitive experiments (table 1), in which the all-sky radiative fluxes over (105°–125°E, 20°–35° N, see the box of figure 1(a)) are set equal to their clear-sky counterparts in shortwave (NS), longwave (NL) and net radiative (NR) calculations, respectively.

[6] www.cloudsat.cira.colostate.edu/dataSpecs.php.

In addition, a control run without these changes is performed (CNTL). Results from three sensitive experiments are then compared to the control run. All experiments are run with 30 vertical levels and a horizontal resolution of 2° and forced by the same prescribed climatological sea surface temperatures (SSTs). All experiments are run 6 years; the outputs of the last 5 years are used in the analysis (see table 1). In order to better compare with satellite observations, the Cloud Feedback Model Intercomparison Project Observation Simulator Package (COSP) (Kay *et al* 2012) is configured in this study.

3. Results

The spatial patterns of the summer mean precipitation and winds (figure 1(a)) show the subtropical high with its southwesterly winds prevailing on Southeastern China, which carries abundant moisture from the South China Sea to Southeastern China at 850 hPa (figure 1(a)). The rain belt is consistent with the wind field, which extends along the Mei-Yu frontal area (~30°N) from the Yangtze River valley to southern Japan.

Consistent with the EASM horizontal circulation, the vertical EASM circulation replaces the domination of Hadley cell over southeastern China (Ye and Yang 1979, Zhou and Li 2002). A prominent feature of the vertical EASM circulation is that a strong updraft accompanied with its southward upper outflow prevails at southeastern China (figure 2(a)). Correspondingly, the seasonal mean rain belt is well synchronized with the updraft, which moves northward beyond 20° N (figure 2(a)).

Following the updraft of the vertical EASM circulation, high clouds dominate Southeastern China (105°–125°E, 20°–35°N) during the summer. The contoured frequency by altitude diagrams (CFAD) of radar reflectivity for cloudy profiles over southeastern China derived from CloudSat/CALIPSO is shown in figure 3(a). As the minimum detectable signal of the Cloud Profiling Radar is −30 dBZ, only results with a reflectivity larger than −30 dBZ are shown. A strong, while narrow, radar reflectivity range extends to high altitudes (12 km). It indicates that the prevailing of anvils is mainly constituted by small ice crystals. The strong and unbroken frequency belt appears from 1 km to 14 km, representing the existence of

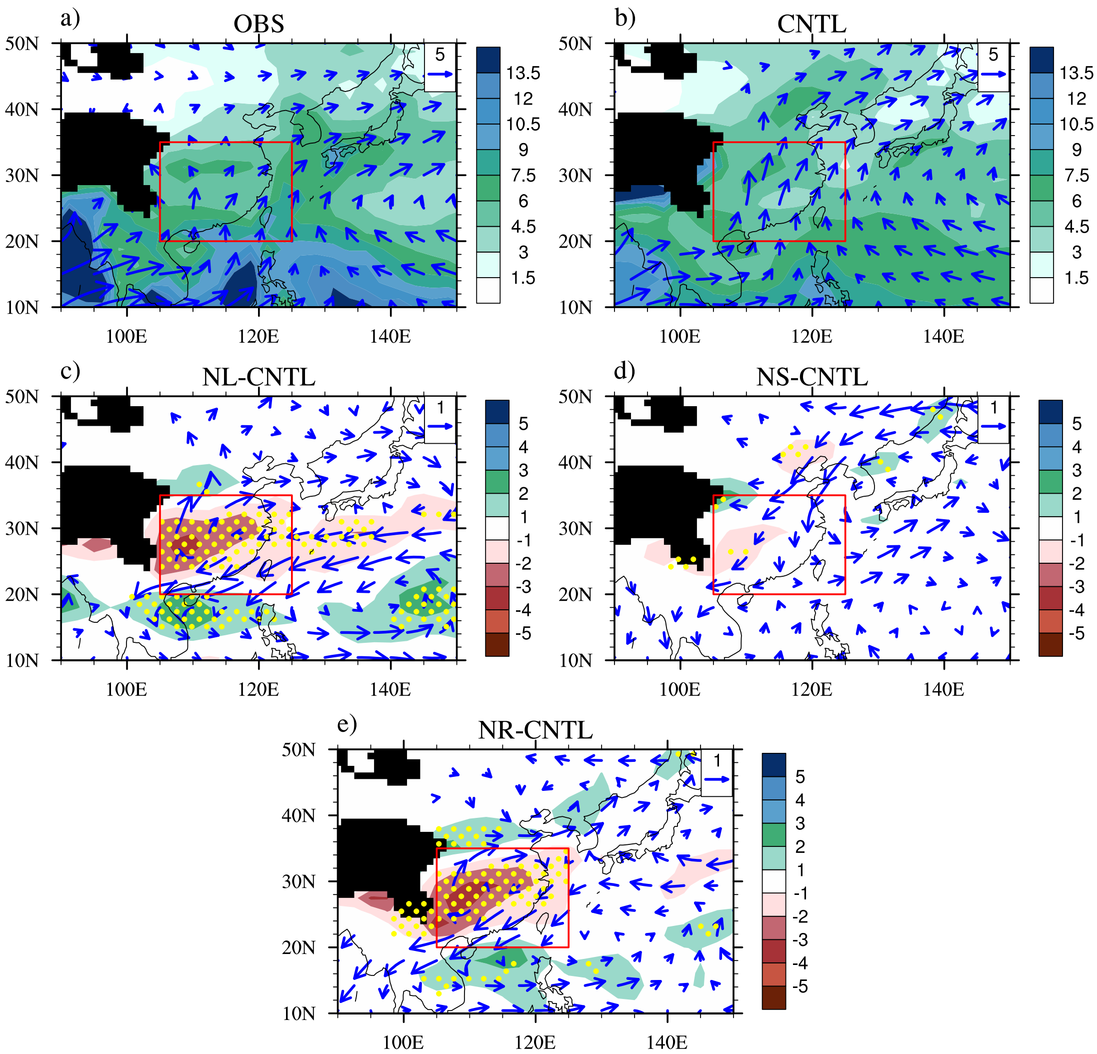

Figure 1. The horizontal distributions of Precipitation (shading, units: mm day^{-1}) and 850 hPa winds (vectors, units: m s^{-1}) in JJA during 1979–2011. (a) Observations (NCEP2 and CMAP), (b) CNTL run, (c) differences between NL and CNTL runs, (d) and (e) are the same as (c), but for NS and NR runs separately. The dotted areas indicate that the precipitation anomalies are statistically significant at the 10% level. The masked areas mean that the topography is higher than 1.5 km. The red boxes are southeastern China (105°–125°E, 20°–35°N).

convective clouds (Luo *et al* 2009). The high frequencies of radar reflectivity above freezing level (4 km) indicate large ice-phase cloud particles. While the frequency belt between −5 dBZ and 10 dBZ below 4 km are probably due to raindrops and liquid-phase cloud droplets.

CAM5 generally reproduces the 3D structures of EASM circulation and cloud system (figure 2(b)). It is notable that the simulated location of western Pacific subtropical high shifts northward relative to the observation (figure 1(b)). Moreover, the simulated vertical circulation of EASM is broader and higher than the observation, and the rain belt is located at the North China Plain (~40°N) instead of the Yangtze River valley (~30°N) (figure 2(b)). Consequently, the simulated radar reflectivity frequency belt vertically penetrates into a higher altitude and covers a wider range (figure 3(b)), which mean more clouds (both liquid- and ice-phase) and higher cloud tops are produced by CAM5.

Figures 1–4 show that clouds play a significant role in influencing the structure and magnitude of EASM by changing the vertical profiles of radiation, including circulation and precipitation. When the cloud longwave radiative effects are ignored (NL run), the weak cloud greenhouse effect causes a negative temperature anomaly of 0.8 K at the mid-level of the troposphere, which further enhances the stability and triggers an anomalous subsidence over southeastern China (figure 2(c)). The strong anomalous subsidence thus results in several responses in the local EASM circulation and precipitation. First, the anomalous subsidence reduces the lifting condensations and cloud occurrence frequency, as the negative anomalous frequencies of cloud radar reflectivity indicates reduction in cumulus and anvils (figure 3(c)). Second, the

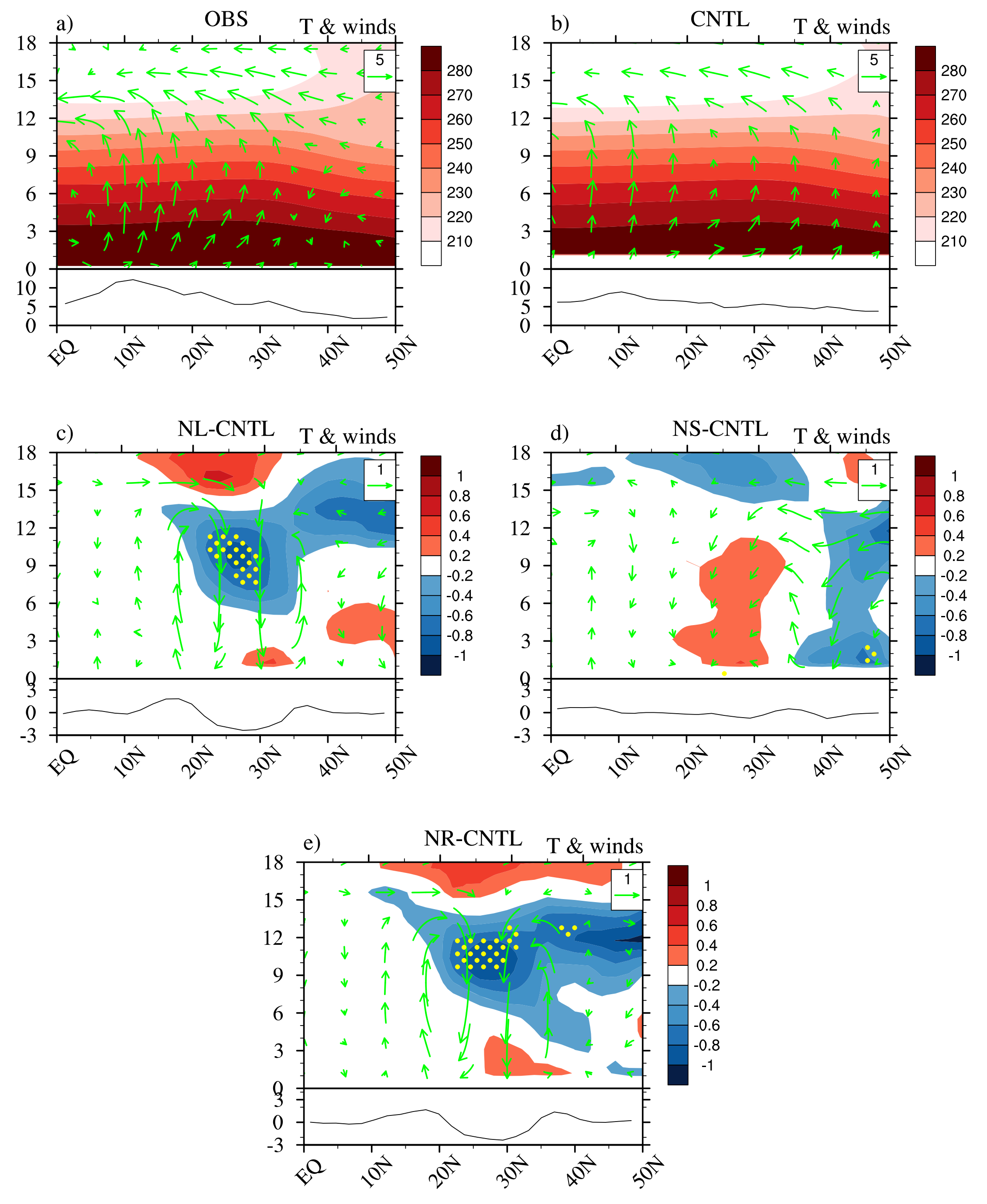

Figure 2. Upper part in each panel: height-latitude cross-section of JJA mean temperature (shading, units: K) and winds (vectors, units: m s^{-1}) averaged over (105°–125°E). Lower part in each panel: latitudinal profile of rainfall based on the same region (unit: mm day^{-1}). (a) Observations, (b) CNTL run, (c) differences between NL and CNTL runs, (d) and (e) are the same as (c), but for NS and NR runs separately. The dotted areas indicate that the temperature anomalies are statistically significant at the 10% level.

anomalous subsidence also produces an anomalous anticyclone located in southeastern China and cyclone appears in the western North Pacific. Their northeasterly winds dominate southeastern China, which cuts down the prevailing moisture transports from the South China Sea at 850 hPa, as shown in figure 1(c). This results in a negative anomalous precipitation in southeastern China and a positive anomalous precipitation in tropical oceans (figure 1(c)).

The responses of circulation and precipitation to the shortwave cloud heating over southeastern China are weaker than those to the longwave cloud heating (figure 1(d)). Ignoring shortwave cloud heating causes warmer conditions at low- and mid-levels that tends to enhance the local instability, however, the changes in temperature are weak (figure 2(d)). Therefore, the cloud longwave radiative heating dominates the overall cloud radiative impacts on EASM circulations (figure 1(e)).

Why does the local cloud radiative heating lead to such a huge impact on the EASM circulation over southeastern China? We use thermodynamic energy

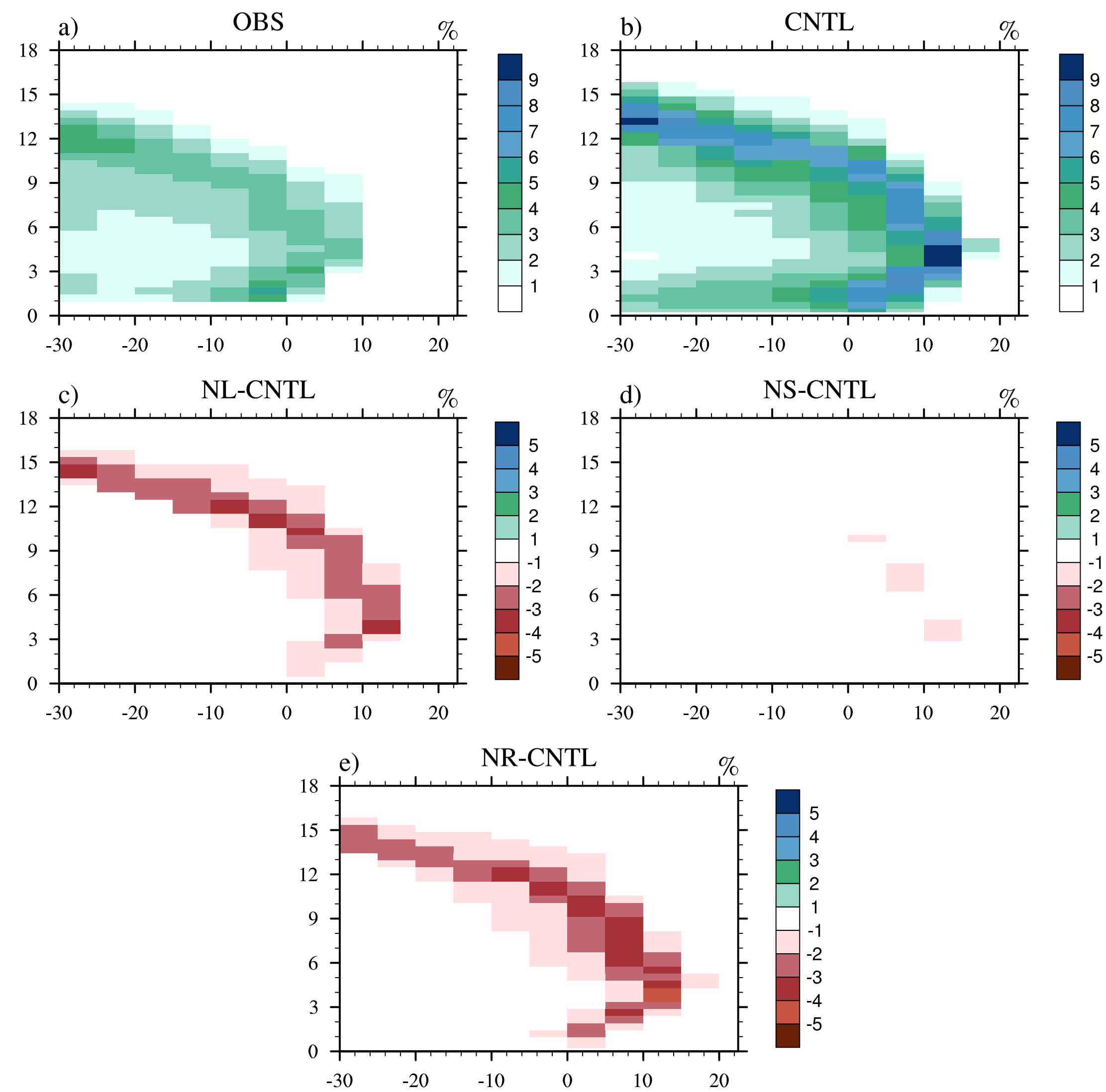

Figure 3. CFAD of JJA mean radar reflectivity averaged over (105°–125°E, 20°–35°N), horizontal coordinate is radar reflectivity (dBz) and vertical coordinate is height. The bin size is 5 dBZ in the horizontal and 0.5 km in the vertical. (a) Observations (CloudSat/CALIPSO), (b) CNTL run, (c) differences between NL and CNTL runs, (d) and (e) are same with (c), but for NS and NR runs separately.

equation and Sverdrup vorticity balance to explain the response in general circulation to the absence of radiative heating.

Ignoring horizontal advection, the thermodynamic energy equation can be simplified as (Ackerman *et al* 1988, Mather *et al* 2007):

$$w\frac{N^2H}{R} = Q \tag{1}$$

where Q represents the heating rates, w means the vertical velocity and H is the scale height. The Brunt-Vaisala frequency is defined by $N^2 = \frac{g}{\theta}\frac{\partial\theta}{\partial z}$, where θ is potential temperature. Equation (1) shows that the radiative heating is balanced by the adiabatic cooling associated with the updraft. In other words, the absence of cloud radiative heating tends to produce an anomalous subsidence.

Over southeastern China, the cloud radiative heating is generally reproduced by CAM5 (figures 4(a) and (b)). However, CAM5 shows the averaged net radiative heating rate caused by clouds is approximately 0.55 K day^{-1} at 6 ~ 12 km, which is larger than 0.47 K day^{-1} in observation (figures 4(a) and (b)). Moreover, the simulated location of the maximum radiative heating is higher compared with observations, which is consistent with the vertical profiles of cloud and EASM circulation (figures 2 and 3). When the cloud radiative effects are ignored (NR run), there is a radiative cooling anomaly of about −0.5 K day^{-1} compared with the control run (figure 4(c)) and most of this anomaly comes from the longwave cloud radiative effects (not shown), similar to what we found in figures 1–2. Based on equation (1), such a radiative deficit generates an anomalous subsidence rate of about 8 hPa day^{-1} with its peak appearing at around 6 ~ 8 km, where the maximum radiative cooling occurs (figure 4(c)). This contributes substantially to EASM circulation, since the updraft of EASM

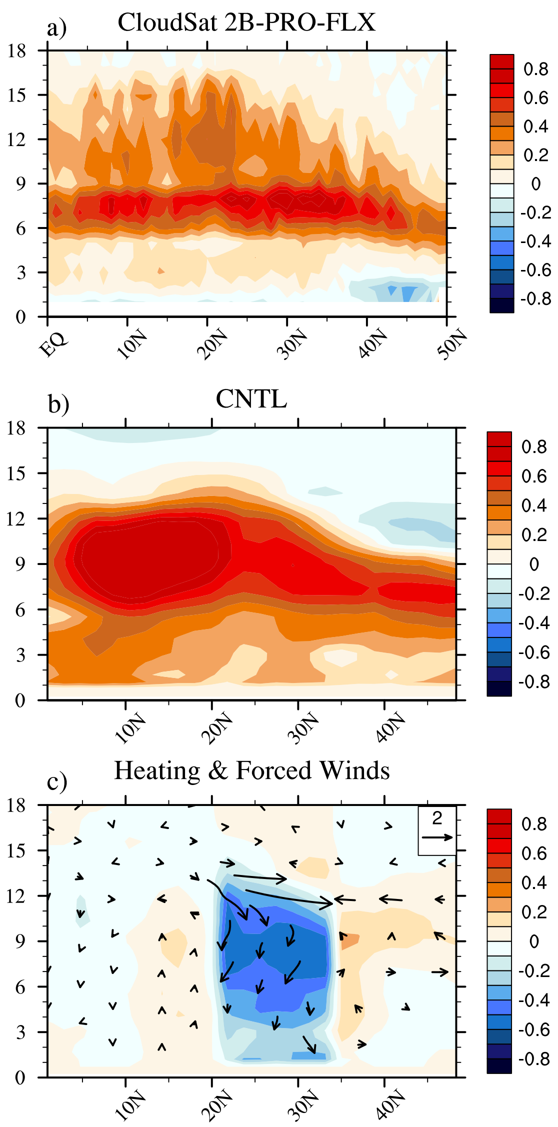

Figure 4. Latitude-height cross-section of JJA cloud radiative heating rates (shading, units K day^{-1}) (a) CloudSat; (b) CNTL run; (c) differences between NR and CNTL runs. The vectors (units m s^{-1}) in (c) show the winds caused by cloud radiative heating by using equations (1) and (2).

circulation is about -20 hPa day^{-1} over southeastern China in CAM5.

The changes in southward upper outflow of EASM can be explained by Sverdrup vorticity balances (Zhou *et al* 2009), that a meridional wind (v) tends to respond to the subsidence caused by cloud radiative cooling anomaly. The Sverdrup vorticity balance is (Rodwell and Hoskins 2001):

$$\beta v = f\frac{\partial \omega}{\partial p} \qquad (2)$$

where $f = 2\Omega \sin\varphi$ is the Coriolis parameter, $\beta = \frac{2\Omega \cos\varphi}{a}$ is its meridional gradient and $\frac{\partial \omega}{\partial p}$ represents vertical velocity gradient of omega. Thus, northward winds are generated above the maximum center of cloud radiative cooling anomaly, because of the positive vertical gradient of omega ($\frac{\partial \omega}{\partial p} > 0$) (figure 4(c)). The vertical circulation forced by cloud radiative cooling anomaly has the opposite structure to EASM circulation (figure 4(c)).

4. Conclusion

Based on the sensitivity experiments of CAM5 model, we show evidence that the cloud radiative heating over southeastern China (105°–125°E, 20°–35°N) has significantly positive impacts on the local EASM circulation and precipitation. When cloud radiative heating is ignored over southeastern China, the model produces an anomalous subsidence and a negative temperature anomaly. Meanwhile, anomalous anticyclone and cyclone occur in southeastern China and the western North Pacific, respectively, which block the low level moisture transport from tropical oceans. These result in a weak EASM. This is because cloud heats the atmosphere at cloud base and cools the atmosphere at cloud top. Based on thermodynamic energy equation, absence of cloud radiative heating induces an anomalous radiative cooling of -0.5 K day^{-1} at the mid-level troposphere, which increases the atmospheric stability and would be balanced by a strong anomalous subsidence of about 8 hPa day^{-1}. The anomalous subsidence subsequently reduces the occurrence frequency of cloud and precipitation and results in a local anomalous anticyclone and a weak subtropical high. Moreover, it further reduces the meridional wind through Sverdrup vorticity balance at high levels of the troposphere. The anomalous vertical circulation caused by absence of cloud radiative heating is opposite to EASM vertical circulation. Therefore, cloud radiative heating leads to a positive effect on the EASM.

Our results imply that clouds and their radiative heating over southeastern China are also significant factors in the simulations of EASM. Bias in clouds may lead to significant bias in simulating EASM circulation and precipitation. Clarifying the importance of cloud radiative heating will not only provide a useful understanding of EASM, but also a possible way to reduce the bias in the simulation of EASM.

Acknowledgements

This work is supported by the National Natural Science Foundation of China under grant 41405103, 41330423 and the National Science Fund for Distinguished Young Scholars under grant 41125017. MW is supported by the Jiangsu Specially-appointed professorship grant. The contribution of authors from PNNL in this manuscript are supported by the US Department of Energy, Office of Science, Biological and Environmental Research, as part of the Earth System Modeling Program. The Pacific Northwest National Laboratory is operated for DOE by Battelle

Memorial Institute under contract DE-AC06-76RLO1830.

References

Ackerman T P, Liou K N, Valero F P J and Pfister L 1988 Heating rates in tropical anvils *J. Atmos. Sci.* **45** 1606–23

Ding Y and Chan J 2005 The East Asian summer monsoon: an overview *Meteorol. Atmos. Phys.* **89** 117–42

Gettelman A *et al* 2010 Global simulations of ice nucleation and ice supersaturation with an improved cloud scheme in the community atmosphere model *J. Geophys. Res.* **115** 216

Iacono M J, Mlawer E J, Clough S A and Morcrette J J 2000 Impact of an improved longwave radiation model, RRTM, on the energy budget and thermodynamic properties of the NCAR community climate mode, CCM3 *J. Geophys. Res.* **105** 14873–90

Kanamitsu M *et al* 2002 Ncep-doe amip-ii reanalysis (r-2) *Bull. Amer. Meteor. Soc.* **83** 1631–43

Kay J E *et al* 2012 Exposing global cloud biases in the community atmosphere model (cam) using satellite observations and their corresponding instrument simulators *J. Clim.* **25** 5190–207

Luo Y, Zhang R and Wang H 2009 Comparing occurrences and vertical structures of hydrometeors between Eastern China and the Indian monsoon region using cloudSat/CALIPSO data *J. Clim.* **22** 1052–64

Mather J H, McFarlane S A, Miller M A and Johnson K L 2007 Cloud properties and associated radiative heating rates in the tropical western Pacific *J. Geophys. Res.* **112** D05201

Mlawer E J, Taubman S J, Brown P D, Iacono M J and Clough S A 1997 RRTM, a validated correlated-k model for the longwave *J. Geophys. Res.* **102** 16663–82

Neale R B *et al* 2011 Description of the NCAR community atmosphere model (CAM 5.0) *NCAR Technical Note* NCAR/TN-4861STR, 1982

Neale R B, Richter J H and Jochum M 2008 The impact of convection on ENSO: From a delayed oscillator to a series of events *J. Clim.* **21** 5904–24

Park S and Bretherton C S 2009 The university of Washington shallow convection and moist turbulence schemes and their impact on climate simulations with the community atmosphere model *J. Clim.* **22** 3449–69

Park S, Bretherton C S and Rasch P J 2014 Integrating cloud processes in the community atmosphere model *J. Clim.* **27** 6821–56

Rodwell M J and Hoskins B J 2001 Subtropical anticyclones and summer monsoons *J. Clim.* **14** 3192–211

Stephens G L *et al* 2002 The cloudsat mission and the a-train *Bull. Amer. Meteor. Soc.* **83** 1771–90

Wang B and Li T 2004 East Asian monsoon—ENSO interaction *East Asian Monsoon* ed C-P Chang (Singapore: World Scientific) 172–212

Wang B, Wu Z, Li J, Liu J, Chang C P, Ding Y and Wu G 2008 How to measure the strength of the East Asian summer monsoon *J. Clim.* **21** 4449–63

Xie P and Arkin P 1996 Analyses of global monthly precipitation using gauge observations, satellite estimates and numerical model predictions *J. Clim.* **9** 840–58

Ye D Z and Yang G 1979 Mean meridional circulations over East Asia and the Pacific Ocean. I: summer; II: winter *Chin. J. Atmos. Sci. Sci.* **3** 299–305

Yu R, Yu Y and Zhang M 2001 Comparing cloud radiative properties between the eastern China and the Indian monsoon region *Adv. Atmos. Sci.* **18** 1090–102

Zhang G J and McFarlane N A 1995 Sensitivity of climate simulations to the parameterization of cumulus convection in the Canadian Climate Centre general circulation model *Atmos. Ocean* **33** 407–46

Zhou T *et al* 2009 Why the Western Pacific subtropical high has extended Westward since the Late 1970s *J. Clim.* **15** 2199–215

Zhou T and Li Z 2002 Simulation of the East Asian summer monsoon using a variable resolution atmospheric GCM *Clim. Dyn.* **19** 167–80